Deformation mechanisms and strain localization in ultramafic rocks: insights from the Balmuccia and Finero peridotites, Ivrea-Verbano Zone

Hadiseh Mansouri[1]*, Ramin Elyaszadeh[2], Virginia Toy[2], Mattia Pistone[3], John Wheeler[4], Sheng Fan[6]

[1]Ruhr Universität Bochum, Germany, [2]Johannes Gutenberg-Universität Mainz, Germany, [3]University of Georgia, USA, [4]University of Utrecht, Netherlands, [5]Liverpool University, UK, [6]University of Otago, New Zealand

*Email: Hadiseh.Mansouri@ruhr-uni-bochum.de

Introduction

The Finero and Balmuccia peridotites, located in the Ivrea-Verbano Zone of the Southern Alps (Fig. 1), are classic examples of mantle-derived ultramafic bodies that have experienced complex magmatic and tectonic histories. Both massifs host abundant pyroxenite dykes, which provide insights into melt–rock interaction and mantle metasomatism.

In this study, we investigate the microstructural relationships between these pyroxenite dykes and their peridotitic host rocks, with a focus on olivine and pyroxene textures, crystallographic preferred orientations (CPOs) and deformation microstructures The aim is to better understand the mechanical and chemical coupling between dykes and surrounding peridotite, and to constrain the generation, coalescence, and migration of melts within the lithospheric mantle.

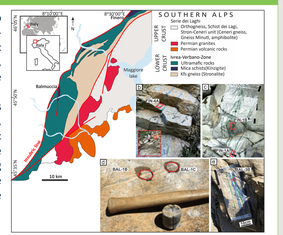

Fig. 1. (a) Geological map of the Ivrea-Verbano Zone (IVZ) showing the main lithotectonic units. Photographs of field exposures showing the sampled banded peridotites from both the (b,c) Finero and (d,e) Balmuccia massifs. The pyroxenite dikes in these images are highlighted by tracing onto an overlain plastic sheet - these tracings were used to document the precise geometric relationships at the sampling sites.

Methodology

Chemical analysis

The chemical compositions of minerals were determined using Electron Probe Microanalysis (EPMA) on a JEOL JXA-8200 at Johannes Gutenberg University, Mainz at an accelerating voltage of 15 keV, with a beam current of 10 nA.

Geothermometry

Temperatures were calculated using microprobe data and several established geothermometers, including the two-pyroxene thermometers of Wells (1977) (T_W77), Brey & Köhler (1990) (T_BKN), Taylor (1998) (T_Ta98), and Bertrand & Mercier (1985) (T_B&M85); the single-clinopyroxene thermometer of Nimis & Taylor (2000) (T_N&T(00)-cpx); the Ca-in-orthopyroxene thermometer of Brey & Köhler (1990) (T_BKN-opx); the olivine–spinel thermometer of Ballhaus et al. (1991) (T_B91(ol)-sp); and the orthopyroxene–spinel thermometers of Liermann & Ganguly (2003) (T_L&G(03)-opx-sp), and Witt-Eickschen & Seck (1991) (T_W-E&S(90)-opx-sp).

EBSD data acquisition and processing

EBSD data were acquired at the University of Utrecht, employing a Zeiss Gemini 450 with an Oxford Instruments Symmetry detector, and 20 keV beam current. EBSD data were analyzed in Channel 5.

We used the **Weighted Burgers Vector (WBV)** method, as introduced by Wheeler et al. (2009), to analyze grain distortion and assess the active slip systems from EBSD data. WBV measures the density of dislocation lines intersecting the plane of interest in 2D, multiplied by their associated Burgers vector(s), and is expressed in units of (length)$^{-1}$.

High-angular resolution electron backscatter diffraction (HR-EBSD) data acquisition and processing

We used HR-EBSD to map geometrically necessary dislocations (GND) and intragranular stress heterogeneity within olivine grains. The HR-EBSD technique employs cross-correlation methods to detect subtle shifts in diffraction patterns, enabling precise mapping of elastic strain, lattice rotations, and residual stresses (Wallis et al., 2021). Five high-resolution EBSD (HR-EBSD) maps (100 × 100 µm each) were collected from olivine grains at various locations within the samples, using a step size of 0.5 µm. Data processing and remapping were performed using the CrossCourt 4 software package at Utrecht University.

References

Ballhaus, C., Berry, R., & Green, D. (1991). High pressure experimental calibration of the olivine-orthopyroxene-spinel oxygen geobarometer: implications for the oxidation state of the upper mantle. *Contributions to mineralogy and Petrology, 107*,27-40.

Bertrand, P., & Mercier, J.-C. C. (1985). The mutual solubility of coexisting ortho-and clinopyroxene: toward an absolute geothermometer for the natural system? *Earth and Planetary Science Letters, 76*(1-2), 109-122.

Brey, G. P., & Köhler, T. (1990). Geothermobarometry in four-phase lherzolites II. New thermobarometers, and practical assessment of existing thermobarometers. *Journal of Petrology, 31*(6), 1353-1378.

Girnis, A. V., & Brey, G. P. (1999). Garnet-spinel-olivine-orthopyroxene equilibria in the FeO-MgO-Al 2 O 3-SiO 2-Cr 2 O 3 systems; II, Thermodynamic analysis. *European Journal of Mineralogy, 11*(4), 619-636.

Hidas, K., Borghini, G., Tommasi, A., Zanetti, A., & Rampone, E. (2021). Interplay between melt infiltration and deformation in the deep lithospheric mantle (External Liguride ophiolite, North Italy). *Lithos, 380*, 105855.

Liermann, H., & Ganguly, J. (2003). Fe 2+–Mg fractionation between orthopyroxene and spinel: experimental calibration in the system FeO–MgO–Al 2 O 3–Cr 2 O 3–SiO 2, and applications. *Contributions to mineralogy and Petrology, 145*, 217-227.

Long, H., Weidner, D. J., Li, L., Chen, J., & Wang, L. (2011). Deformation of olivine at subduction zone conditions determined from in situ measurements with synchrotron radiation. *Physics of the Earth and Planetary Interiors, 186*(1-2), 23-35.

Nimis, P., & Taylor, W. R. (2000). Single clinopyroxene thermobarometry for garnet peridotites. Part I. Calibration and testing of a Cr-in-Cpx barometer and an enstatite-in-Cpx thermometer. *Contributions to mineralogy and Petrology, 139*, 541-554.

Sudholz, Z. J., Yaxley, G. M., Jaques, A. L., & Brey, G. P. (2021). Experimental recalibration of the Cr-in-clinopyroxene geobarometer: improved precision and reliability above 4.5 GPa. *Contributions to mineralogy and Petrology, 176*, 1-20.

Taylor, W. (1998). An experimental test of some geothermometer and geobarometer formulations for upper mantle peridotites with application to the thermobarometry of fertile lherzolite and garnet websterite. *Neues Jahrb. Mineral. Abh., 172*, 381-408.

Wallis, D., Hansen, L. N., Wilkinson, A. J., & Lebensohn, R. A. (2021). Dislocation interactions in olivine control postseismic creep of the upper mantle. *Nature Communications, 12*(1), 3496.

Wells, P. R. (1977). Pyroxene thermometry in simple and complex systems. *Contributions to mineralogy and Petrology, 62*(2), 129-139.

Wheeler, J., Mariani, E., Piazolo, S., Prior, D., Trimby, P., & Drury, M. (2009). The weighted Burgers vector: a new quantity for constraining dislocation densities and types using electron backscatter diffraction on 2D sections through crystalline materials. *Journal of microscopy, 233*(3), 482-494.

Witt-Eickschen, G., & Seck, H. (1991). Solubility of Ca and Al in orthopyroxene from spinel peridotite: an improved version of an empirical geothermometer. *Contributions to mineralogy and Petrology, 106*, 431-439.

General microstrucutres of the studies samples

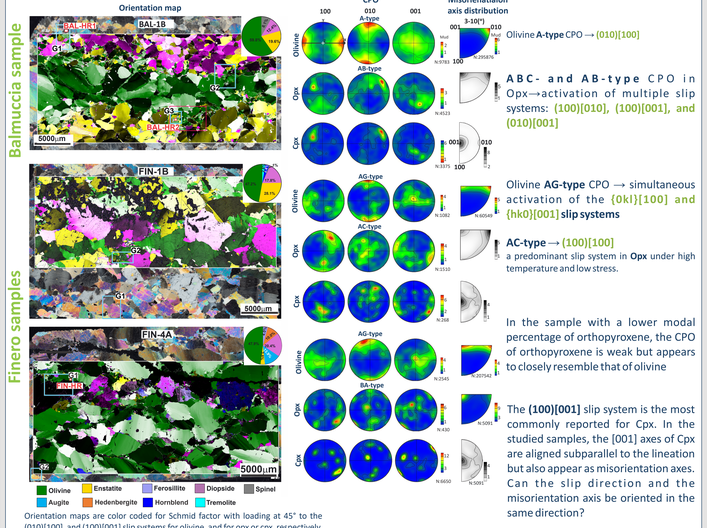

Orientation maps are color coded for Schmid factor with loading at 45° to the (010)[100], and (100)[001] slip systems for olivine, and for opx or cpx, respectively. Areas marked with letter G indicate the EPMA analysis locations.

Olivine **A-type** CPO → (010)[100]

ABC- and AB-type CPO in Opx→activation of multiple slip systems: (100)[010], (100)[001], and (010)[001]

Olivine **AG-type** CPO → simultaneous activation of the {0kl}[100] and {hk0}[001] **slip systems**

AC-type → (100)[100]
a predominant slip system in **Opx** under high temperature and low stress.

In the sample with a lower modal percentage of orthopyroxene, the CPO of orthopyroxene is weak but appears to closely resemble that of olivine

The **(100)[001]** slip system is the most commonly reported for Cpx. In the studied samples, the [001] axes of Cpx are aligned subparallel to the lineation but also appear as misorientation axes. Can the slip direction and the misorientation axis be oriented in the same direction?

Grain distortion and WBV analysis for some Opx and Cpx grains

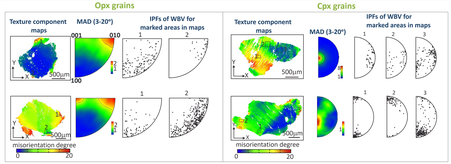

Given the orientation of WBVs, the activation of [100] and [010] slip systems in Opx and Cpx grains is plausible.

Boundary hierarchy characteristics

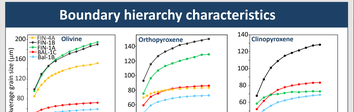

Olivine grains display a relatively discontinuous boundary hierarchy.
Does the steeper slope in this chart indicate a higher frequency of subgrain boundaries—and thus greater internal deformation—in olivine grains from the Finero samples compared to those from Balmuccia?

Paleopiezometry

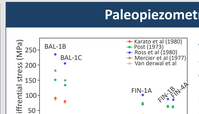

Relationship between grain size and differential stress for olivine

The piezometer of Karato et al. (1980) suggests that the differential stress in the Balmuccia and Finero peridotites is approximately 73 ± 5 MPa and 30 ± 2 MPa, respectively.

Crystallographic and chemical relationships between recrystallized grains and their parent grains

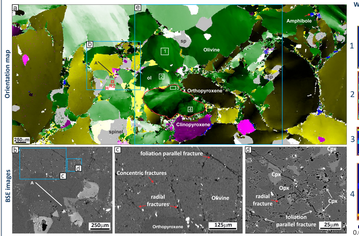

The WBV vectors suggest that both [100] and [001] dislocations contribute to the formation of olivine subgrain boundaries in the contact regions.

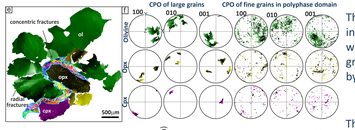

The crystallographic orientations of fine-grained minerals in the polyphase domain are dispersed around, and aligned with, the orientations of their adjacent larger or parent grains, indicating they are derived from those larger grains by a subgrain rotation recrystallization process?

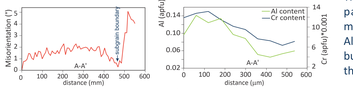

The misorientation profile along transect A–A' *The chemical profile along transect A–A'*

The misorientation profile along transect A–A', from an Opx parent grain to the attached bulge, reveals a 5° misorientation between the bulge and its parent grain. Along the A–A' transect, chemical profiles indicate that the bulge has lower concentrations of Al and Cr compared to the parent grain.

HR-EBSD data

FIN-HR1: Olivine is in contact with clinopyroxene rich layer
BAL-HR1: Olivine is in contact with clinopyroxene grain
BAL-HR2: Olivine is in the center of the olivine rich layer
BAL-HR3: Olivine is in contact with the orthopyroxene rich layer
BAL-HR4: Olivine is in contact with an orthopyroxene grain

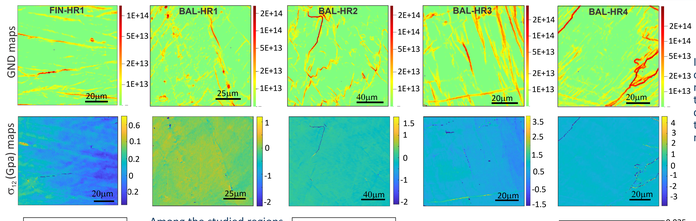

In sub-areas, where olivine is in contact with opx grains, the stress magnitudes are higher, ranging from 3 to 4 GPa in bands with elevated GND density. These stresses are higher than those typically expected for the mantle lithosphere

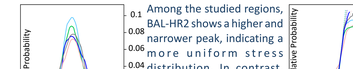

Among the studied regions, BAL-HR2 shows a higher and narrower peak, indicating a more uniform stress distribution. In contrast, BAL-HR3 displays a broader distribution, suggesting greater variability in stress within this region.

The tails related to high stress magnitudes deviate from the straight lines. These deviations indicate a departure from normality in the high-stress regions.

Stress distributions generated by dislocations typically follow a power-law decay, $P(\sigma_{12}) \propto \sigma_{12}^{-3}$, which appears as a straight-line relationship in the restricted second moments (γ_2) plot (Wallis et al., 2021).

Mineral chemistry

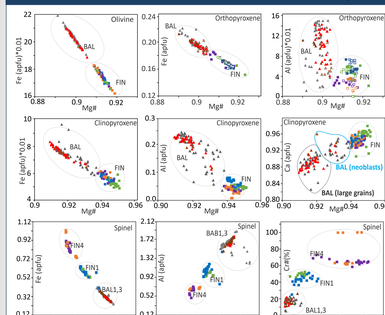

The lack of sharp chemical gradients in Mg# and Fe contents of the olivine and Opx grains is typically attributed to high-temperature chemical equilibration by diffusion and/or prior buffering of the melt composition to match that of the host peridotite(Hidas et al., 2021).

Spinels from the Finero peridotite are characterized by high Cr# values (> 0.4) and elevated TiO_2 contents (0.5 to 2 wt.%), which are typical of peridotites that have interacted with melts in suprasubduction zone settings(e.g. Karimov et al., 2020). Spinels in the Balmuccia peridotite are predominantly aluminum-rich (Al-spinel), indicating formation under anhydrous conditions influenced by high-temperature, aluminum-rich melts.

Geothermometry - discussion points

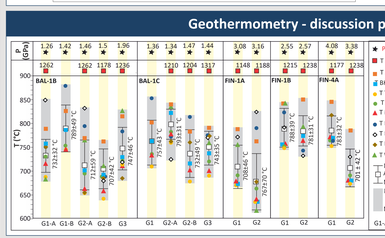

Can the Cr-in-clinopyroxene barometer calibrated by Sudholz et al. (2021) be applied to our peridotite samples, which do not contain garnet? This calibration is based on Cr exchange between clinopyroxene and garnet.

The thermometer calibration by Girnis et al. (1999) is based on Fe-Mg exchange between spinel and orthopyroxene in garnet peridotites. Is this calibration suitable for our samples?

Conclusions

- Microstructural analysis suggests that prior to melt infiltration, olivine grains deformed by dislocation creep and subgrain rotation (SGR). The presence of an A-type CPO indicates deformation under high-temperature (>1000 °C), dry conditions, and an estimated stress of around 73 ± 5 MPa.
- The parallelism between the pyroxenite layers and the foliation in the host peridotite, along with consistent microstructures and CPO patterns in olivine and pyroxene grains, suggests synkinematic Al-rich melt infiltration and replacement of olivine by pyroxenes.
- Olivine deforms by dislocation creep, typically activating the [100] slip system under dry conditions. However, in the presence of melt, the [001] slip system becomes active in olivine, facilitating its transformation into orthopyroxene and clinopyroxene. This is consistent with [001] being the easiest slip system in pyroxenes, suggesting crystallographic inheritance during the phase transformation.
- The AG-type CPO in olivine, along with AC- and BA-type CPOs in orthopyroxene and the presence of Cr-spinel in the Finero samples, suggest melt-assisted deformation facilitated by an H_2O-rich influx.